Separating atmospheric layers in adaptive optics

Erez N. Ribak

Department of Physics, Technion, Haifa 32000, Israel, and
Center for Adaptive Optics, University of California, Santa Cruz, California 95064

Received November 26, 2002

Several optical schemes have been proposed to measure the separate contributions of atmospheric layers for astronomical adaptive optics. I show here that simple conjugation of the wave-front sensors to the layers is sufficient. Although a larger camera is required for a larger field of view, only the pixels that sense stars are being read out. The nearly periodic Hartmann data are analyzed by Fourier filtering so that the signals from all stars are added up while most of the noise is excluded. Acoustic Hartmann wave-front sensors [Opt. Lett. **26,** 1834 (2001)] that switch between layers improve flexibility and sensitivity. © 2003 Optical Society of America

OCIS codes: 010.1080, 100.6950, 120.5050.

More and more telescopes are now being equipped with adaptive-optics systems. These systems include a wave-front sensor, a wave-front corrector, and a control system to process the measured wave front into commands for the corrector. Such a system can gain a significant field of view by use of more than one sensor and more than one corrector (see the review in Ref. 1). The basic scheme, now under development in some observatories, requires that a few stars be detected with a few matching sensors [Fig. 1(a)] and that the tomographic data that are solved for be processed into commands for the correctors. These correctors are usually optically conjugated to the most disturbing atmospheric layers. In stellar fields lacking nearby stars for this purpose, laser guide stars can be used.

There have also been other approaches in which wave-front measurement is layer oriented rather then star oriented. The first called for creating an ordered grid of bright laser spots or fringes to be detected by a Hartmann–Shack sensor with a wide field of view in each lenslet.[2,3] The resulting periodic pattern in each lenslet focus is Fourier analyzed for gross movement and linked with the lower atmospheric layers; then internal distortions, associated with higher turbulence, are compared among lenslets. A somewhat similar approach is taken in solar adaptive optics.[4]

Direct detection of the layers' turbulence by addition of light crossing these layers is more efficient.[5,6] Use is made of a pyramid wave-front sensor, which can be viewed as two orthogonal knife-edges. The refractive pyramid is placed against the magnified image of the star, providing four gradients of the wave front that correspond to the knife-edges. These gradients are measured in detectors that are conjugate to the atmospheric layers of interest [Fig. 1(b)]. In the multistar version, light from the magnified beacons, each deflected by its corresponding pyramid, is added onto the same layer detector. Thus each point in the detector collects the light from all beacons passing through the conjugate layer. This is an efficient rearrangement of the Hartmann–Shack sensor, since the pixel size can be chosen according to the turbulence strength.

In this method the pyramids are to be moved to locations conjugate to the natural or artificial beacons. However, if a laser fringe pattern is being used as multiple guide stars, it is possible to have a rigid pyramid array and instead match the fringes to it. In this case the pyramids can be replaced with holograms or blazed gratings for steering of the monochromatic light to the corresponding layer detectors.[7] The (incoherent) addition of the laser spots on the layer detectors allows a great reduction in the total laser power required. This is because the total number of detector pixels, which is equal to the sum of isoplanatic patches in the different layers, is not much larger than that for the integrated atmosphere.[1,7]

Assume now that a Hartmann–Shack sensor is optically conjugated to a high atmospheric layer, such that the layer is imaged on the plane of the lenslets. This sensor will yield the wave-front gradients in this layer. By use of a beam splitter, another portion of the incoming beacons' light can be imaged on such a separate sensor. But the lenslets in this second sensor are now conjugated to another layer, providing the wave-front gradients at that layer. As each layer has its typical turbulence, the lenslet pitch in the conjugate to that layer can be made to match its Fried parameter, r_0. More detectors can be added for more layers, each with unique spacing [Fig. 1(c)]. Currently this is achieved by variable magnification or by replacement of rigid lenslet arrays.

Recently, a flexible sensor was developed that imposes the same periodic modulation on the incoming wave front in the same manner as lenslet arrays. This modulation is achieved in the near field of two crossed, standing acoustic waves.[8] When the atmosphere becomes more turbulent, the acoustic period can be increased to better sample it. When turbulence is lower, a longer acoustic period is tuned, since the number of photons per period increases and the relative noise decreases. It is suggested that these flexible sensors be used to measure the different layers, each with its typical turbulence and corresponding acoustic period. Because of the depth available in these flexible wave-front sensors, it is also possible to cascade different acoustic standing waves at different conjugates with the same camera, alternating between the layers. Thus one acoustic array is excited at one

0146-9592/03/080613-03$15.00/0

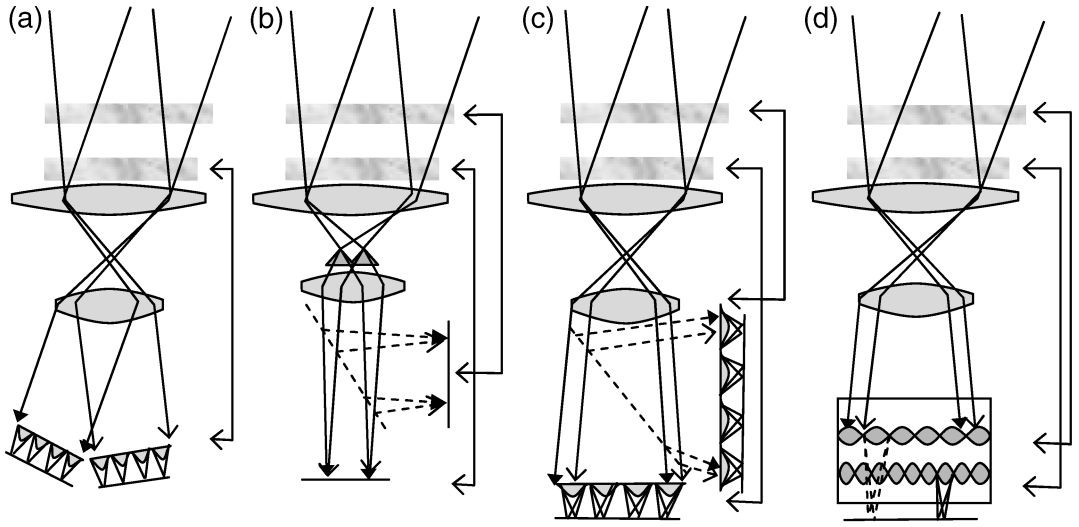

Fig. 1. (a), Different sensors, conjugate to the telescope pupil, allow reconstruction of the atmospheric layers. (b), Pyramids, at the images of the beacons, and detectors, conjugate to the atmospheric layers, directly measure slopes in these layers. (c), Lenslet arrays, conjugate to the atmospheric layers, directly measure slopes in these layers. The lenslets' pitch is matched to the layer turbulence. (d), Two alternating acoustic beams, each conjugate to a different layer, save a beam splitter but halve the detector integration time per layer.

frequency and conjugate to one layer, and its spot pattern with the wave-front slopes is measured. Then this array is switched off, and a lower array, conjugate to the lower layer, is turned on within a few microseconds. The same camera measures the slopes in the second layer at a different frequency, and so on [Fig. 1(d)]. The focal length of these acoustic caustics can be tuned to the distance to the camera by a change in the input power. One can choose the integration time of the different layers to maximize the ratio of signal to noise.

How can these layer-conjugated detectors (rigid or flexible) measure a multiplicity of beacons? Their field of view has to be wide enough to include these beacons, so that in each focal area of each lenslet there are multiple images of the various stars. One can reduce the very large number of pixels necessary to register these images by reading out only the ones near the beacons' images and ignoring the rest of the sky. The global shift of the whole pattern in each lenslet yields the wave-front gradients at the corresponding area of the conjugate layer. Other defocused layers cause minute internal shifts of the stars inside each lenslet that one may trace back to the layer[2,3] to enhance direct measurement of the stars with the conjugate sensor.

It is customary to extract the slope of the wave front by calculation of the centroid in each Hartmann–Shack lenslet. When the flexible array is used, spectral filtering methods are better suited to the application, as they are less sensitive to accurate registration of the focal spots to the detector pixels. The whole spot pattern is transformed, and the directional wave-front gradients are identified as the horizontal and vertical sidelobes of the Fourier spectrum (Fig. 2). Direct commands for the wave-front corrector can now be taken from these two sidelobes.[9] This spectral method also lends itself to use in future large telescopes in which the number of lenslets (rigid or flexible) will be large and the centroiding process slower.

In the case of nearer laser beacons (Rayleigh or sodium layer), an additional shift and additional defocus occur between the images in the different lenslets. The effect of defocus can be somewhat overcome by placement of the camera between the high and low foci to get a similar spot size for stars and laser spots. Then, there are two ways to deal with the image scales of natural and artificial beacons. In the first method the images of all beacons are calculated in each lenslet regardless of their origin. In the second method the natural images and the artificial ones are separated after readout and processed separately

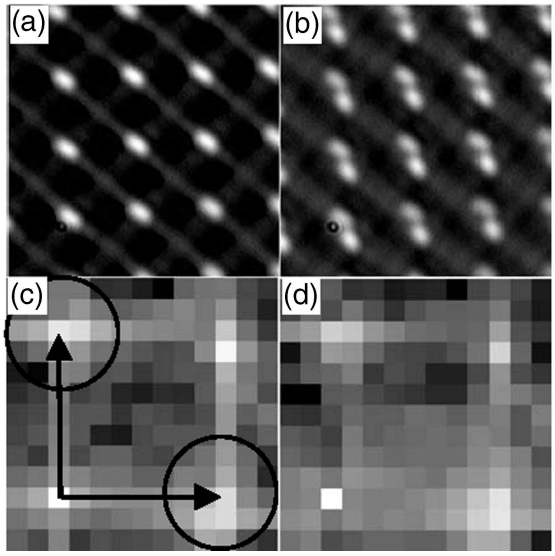

Fig. 2. (a), (b) Hartmann (acoustic) lenslet array images of one object and two objects. (c), (d) Fourier transforms of a and b on a logarithmic scale. The two sidelobes (in circles, at distance D/d from the origin) contain all the slope data.

(empty subfields are skipped for the sake of speed and noise reduction) and pieced together again in two images of the detector spots: natural and artificial. Because the two images have a slightly different spatial frequency, their Fourier transforms will produce the same information but placed radially apart. Thus their corresponding sidelobes can be added together. The pixel where they differ is the central one of each sidelobe: Its phase is the tip and tilt of the wave front as sensed by the two different sets of beacons.[2] It is also possible to measure the natural beacons alone in short periods when the laser is off or through a dichroic mirror. Because the main need for additional natural stars is for global slope and low-order modes, these stars can be measured by a simpler, separate detector.

The spectral method of analysis of the data adds the signals from all pixels, and the Poisson and read noise are evenly distributed over the whole Fourier domain, thus improving the ratio of signal to noise at the spatial frequency band of the lenslets.[10] Suppose that the camera holds $p \times p$ pixels, where each pixel has an angular size on the sky of a fraction $\kappa \leq 1$ of the diffraction spot λ/d rad, the ratio of wavelength to lenslet diameter. Assuming a few stars in the field of view of each lenslet, it is possible to estimate the number of relevant pixels to be read out. Suppose the beacons are spread over a field of Φ^2 rad^2, equivalent to $(\Phi d/\kappa\lambda)^2$ pixels. There are $(D/d)^2$ lenslets inside the telescope aperture (of diameter D), and when multiplied, there are $p^2 = (\Phi D/\kappa\lambda)^2$ pixels all together that are facing all the lenslets. This number of pixels is as if the wide field were measured by the full telescope. Now assume that β beacons are used, natural or artificial, each requiring ϑ pixels across to measure it (with the diffraction spot oversampled, $\kappa\vartheta > 1$). Multiplying by the number of lenslets, one finds that $\mu = \beta(\vartheta D/d)^2$ pixels are to be read out. This result means that these pixels are a small fraction of the whole array: $\mu/p^2 = \beta(\vartheta/\Phi)^2(\kappa\lambda/d)^2$, or the ratio of the combined area of all the beacons to the area of the whole field. For example, four beacons inside a $1'$ field, each measured over eight pixels across in $0.5''$ pixels, require that only 2% of the camera area be read out. These wasted (unread) pixels are the greatest disadvantage of the this scheme. However, if all stars in the field, bright and weak, are measured with larger telescopes, they might provide enough photons to reduce the need for laser beacons.[5]

To appreciate the effect of noise, let us assume that there are N photons from all beacons in one layer-conjugate sensor. The Fourier transform of the spot pattern, also of size $p \times p$, will include all N photons, and in each sidelobe also nearly N photons. The total noise is spread evenly, such that the variance of each Fourier frequency[9] will be $(N + {\sigma_r}^2\mu)/p^2$ arising from the Poisson noise and from lesser read noise of σ_r per pixel. With turbulence, the width of each sidelobe includes all the modes, or degrees of freedom measured. There are two orthogonal sidelobes for the two gradients (the other two are their Hermitian conjugates), and each frequency has two degrees of freedom, its amplitude and phase (Fig. 2). The width of these sidelobes is limited to the distance between them, or else they will contain data from the next sidelobe. Since the lenslet frequency is D/d, the first sidelobes are centered at pixels $\pm D/d$, so D/d is also the bandwidth. Thus the two wave-front slopes are fully described by two sidelobes, each with $(D/d)^2$ independent complex modes. Since nearly the same number of photons N is now divided into that many modes in the sidelobes, each mode gets on the average approximately $N/(D/d)^2$ photons. Thus the average signal-to-noise ratio per mode is $[N/(D/d)^2]/[(N + {\sigma_r}^2\mu)/p^2]^{1/2} = N^{1/2}p(d/D)^2/(1 + {\sigma_r}^2\mu/N)^{1/2}$. However, not all modes are equal. The shape of the sidelobes is the Fourier transform of the wave-front slopes over the telescope aperture[9]; the low modes are higher than this noise level, and the high modes are below it. Notice the strong dependence of the signal on the size d of the lenslets, and hence the advantage of using a layer-dependent sensor with larger d when the turbulence is weaker.

This work was funded by the National Science Foundation Science and Technology Center for Adaptive Optics, managed by the University of California at Santa Cruz under cooperative agreement AST-9876783. The author's e-mail address is eribak@physics.technion.ac.il.

References

1. E. N. Ribak, in *Adaptive Optics Engineering Handbook*, R. K. Tyson, ed. (Marcel Dekker, New York, 2000), and references therein.
2. Y. Baharav, E. N. Ribak, and J. Shamir, Opt. Lett. **14,** 242 (1994).
3. Y. Baharav, E. N. Ribak, and J. Shamir, J. Opt. Soc. Am. A **13,** 1083 (1996).
4. T. Berkefeld, D. Soltau, and O. von der Luhe, Proc. SPIE **4839,** 66 (2002).
5. R. Ragazzoni, J. Farinato, and E. Marchetti, Proc. SPIE **4007,** 1078 (2000).
6. R. Ragazzoni, Proc. SPIE **4840** (to be published).
7. E. Ribak and R. Ragazzoni, Proc. European Southern Observatory **58,** 281 (2001).
8. E. N. Ribak, Opt. Lett. **26,** 1834 (2001).
9. Y. Carmon and E. N. Ribak, Opt. Commun. **215,** 285 (2003).
10. E. N. Ribak, C. Roddier, F. Roddier, and J. B. Breckinridge, Appl. Opt. **27,** 1183 (1988).